Preparation of conductive polyphenylene sulfide/polyamide 6/multiwalled carbon nanotube composites using the slow migration rate of multiwalled carbon nanotubes from polyphenylene sulfide to polyamide 6

Ling Xu, Bo-Yuan Zhang, Zhuo-Yue Xiong, Zhao-Xia Guo, Jian Yu

Key Laboratory of Advanced Materials (MOE), Department of Chemical Engineering, Tsinghua University, Beijing 100084, People's Republic of China

Correspondence to: Z.-X. Guo (E‑mail: guozx@mail.tsinghua.edu.cn) and J. Yu (E‑mail: yujian03@mail.tsinghua.edu.cn)

ABSTRACT: Conductive polyphenylene sulfide (PPS)/polyamide 6 (PA6)/multiwalled carbon nanotube (MWCNT) composites having 10–30 wt % PA6 and 1 wt % MWCNTs are prepared by melt mixing at 300°C for 8 min using a high concentration PPS/MWCNT masterbatch approach, and the migration kinetics of MWCNTs from thermodynamically unfavored PPS to favored PA6 was investigated. The morphology of the composites was investigated by field emission scanning electron microscopy and transmission electron microscopy, showing the localization of most MWCNTs in the PPS phase and at the interface, being different from the case of direct melt mixing where non-conductive materials were obtained with most MWCNTs found in the PA6 phase and at the interface. The electrical resistivity and morphology of the materials as a function of time were investigated, showing that the conductive materials can be prepared within a mixing time of 4–16 min because of the slow migration rate of MWCNTs from PPS toward PA6, and MWCNTs can eventually migrate into the PA6 phase after a long mixing time of 30 min. The slow migration rate of MWCNTs was attributed to the high viscosity ratio of the two phases. This article shows a good example where the migration of MWCNTs was slow enough to control and can be used to prepare conductive polymer blends. © 2015 Wiley Periodicals, Inc. J. Appl. Polym. Sci. **2015**, *132*, 42353.

INTRODUCTION

Mixing polymer blends with carbon fillers such as carbon black (CB) and carbon nanotubes (CNTs) is a viable approach to prepare conductive polymeric materials.[1–34] In most published work, the carbon fillers are selectively localized in one polymer phase or at the interface of blends displaying co-continuous phase morphology. The electrical percolation thresholds are dramatically lowered because of the phenomenon of double percolation.[1,5–14] When blends having sea-island structure are involved, the electrical conductivity usually increases if the carbon filler is selectively localized in the continuous phase due to the increased effective concentration of the carbon filler.[15–17] When the conductive filler is selectively localized in the dispersed phase, the composite material is usually non-conductive unless the interparticle distance is small enough to allow tunneling effect to happen as a result of small particle size and big particle number.[18–21]

The migration of carbon fillers in polymer blends from one polymer phase to another is of both academic and practical interests.[6–8,10,22–29] When a carbon filler is pre-compounded in the thermodynamically unfavored polymer phase, it usually migrate toward the favored phase during melt mixing. For example, multiwalled carbon nanotubes (MWCNTs) migrate from poly(styrene-co-acrylonitrile) (SAN) to polycarbonate (PC),[6] from high density polyethylene (HDPE) to PC or polyamide 6 (PA6)[23] and from poly(lactic acid) (PLA) to poly (ε-caprolactone) (PCL),[7] and functionalized MWCNTs from HDPE to the interface between HDPE and PA6.[24] In addition to thermodynamic factors, there are also kinetic factors that can affect the migration of carbon fillers. The migration process can be controlled by varying mixing time, mixing sequence, or viscosity ratio of the two phases. For example, by controlling mixing time, Gubbels et al.[25] allowed CB to migrate to the interface of 45/55 polyethlene (PE)/polystyrene (PS) blend and Huang et al.[7] managed MWCNTs to the interface of 50/50 PLA/PCL
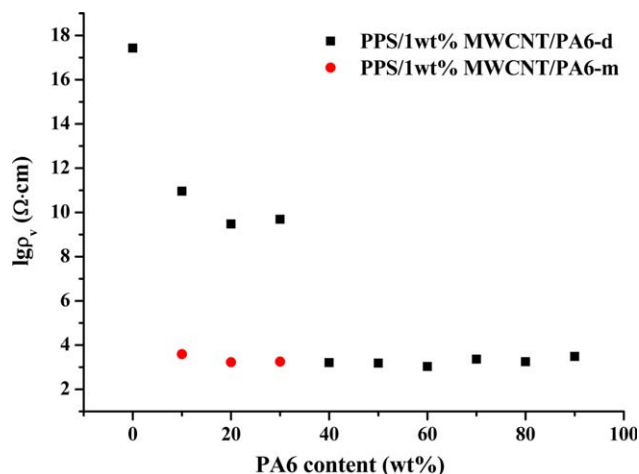
Figure 1. Electrical resistivity of PPS/1 wt % MWCNT/PA6 composite as a function of PA6 content. [Color figure can be viewed in the online issue, which is available at wileyonlinelibrary.com.]

blend, obtaining materials with minimum electrical resistivities. Shi et al.[8] reported that the huge viscosity ratio of poly(L-lactide)/ethylene-co-vinyl acetate (PLLA/EVA) can hinder the migration of CNTs from thermodynamically unfavored EVA to favored PLLA.

Polyphenylene sulfide (PPS)/PA6 blends have good mechanical property, high temperature and wear resistance, and good processability. They are widely used in industry for making packaging materials, household and auto electric appliances, electronic products, pipeline, and so on. It is interesting to prepare conductive PPS/PA6 blends by mixing with CNTs to widen their applications in the electronic field. To the best of our knowledge, conductive CNT-filled PPS/PA6 blends have not been reported. In this work, a masterbatch approach where MWCNTs are pre-compounded into the thermodynamically unfavored PPS is envisaged to obtain conductive PPS/PA6/MWCNT materials, which cannot be obtained by direct melt mixing due to the selective localization of MWCNTs in the dispersed PA6 phase, using the slow migration rate of MWCNTs from PPS to PA6. The migration kinetics is investigated in view of electrical resistivity and morphology of the materials.

EXPERIMENTAL

Materials

The MWCNTs used in the work were supplied by Tsinghua University, China. The purity was above 95 wt %. The diameter of the MWCNTs ranged from 3 to 20 nm with the statistic average diameter of 10 nm, and the length was several micrometers. PPS in a powder form, with a density of 1.33 g/cm^3 and a melt temperature of 280.5°C, and PA6 (1013B), with a density of 1.14 g/cm^3 and a melt temperature of 220°C, were purchased from Sichuan Deyang Chemical Corporation (China) and UBE Industries (Japan), respectively, and dried in a vacuum oven at 120°C for 5 h and 80°C for 12 h, respectively.

Sample Preparation

Direct Method. PPS/PA6/MWCNT composites containing 1 wt % MWCNTs with a wide range of PPS/PA6 compositions, were prepared by melt mixing in a torque rheometer (RM-200A Rheometer, Harbin Hapro Electrical Technology Co., Ltd) at 300°C. The rotation rate was 60 rpm and the mixing time was 8 min unless specified. The composites were denoted as PPS/1 wt % MWCNT/PA6-d.

Masterbatch Method. PPS/MWCNT masterbatch containing 5 wt % MWCNTs was prepared first and then diluted with neat PPS and PA6 to obtain composites with 1 wt % MWCNT loading, denoted as PPS/1 wt % MWCNT/PA6-m. The melt mixing conditions were the same as for direct method.

Characterization

Electrical Resistivity. Prior to the electrical resistivity measurements, all the composites were compressed into plates under a pressure of 8 MPa for 7 min using a hot-press at 300°C. Disk samples with a diameter of 20 mm and thickness of 1.8 mm or diameter of 75 mm and thickness of 0.375 mm were prepared for low and high resistivity measurements, respectively. In brief, samples with higher electrical resistivity ($>10^8$ Ω cm) were measured by the ZC-36 resistivity tests (Shanghai Cany Precision Instrument); and more conductive samples ($<10^8$ Ω cm) were measured using a four-point test fixture (KDY-1, Guangzhou Kunde Co., Ltd). Data from four measurements were averaged.

Field Emission Scanning Electron Microscopy (FESEM). FESEM was performed on a JEOL model JSM-7401 apparatus with an operating voltage of 3.0 kV to investigate the phase morphology. Samples for FESEM observation were cryo-fractured in liquid nitrogen and etched with formic acid at room temperature under ultrasonic for 20 min to remove the PA6 phase.

Transmission Electron Microscopy (TEM). TEM was carried out on a Hitachi H-800 Electron Microscope operating at 200 kV to examine the localization of MWCNTs. Ultrathin sections were made on an ultratome (LKB model 2088; LKB-Producer AB, Bromma, Sweden).

Measurements of Contact Angles. Contact angle measurements were performed with a POWEREACH apparatus (Shanghai Zhongchen Co Ltd., China) to assess the surface tensions of PPS, PA6 used in this work. In general, the surface tension of a solid consists of two parts, the dispersive part and the polar part:

$$\gamma_S = \gamma_s^d + \gamma_s^p \tag{1}$$

The relations between contact angle and surface tension can be described by the Owens method:[35]

$$\gamma_l(1 + \cos\theta) = 2\left(\gamma_s^d \gamma_l^d\right)^{1/2} + 2\left(\gamma_s^p \gamma_l^p\right)^{1/2} \tag{2}$$

where γ_s and γ_l are the surface tensions of the solid and liquid, γ_s^d, γ_s^p, γ_l^d, and γ_l^p are the dispersive and the polar parts of the solid and liquid, and θ is the contact angle. The γ_s, γ_s^d, γ_s^p of the solid can be calculated by combining eqs. (1) and (2) after the contact angle measurements with at least two different liquids.

RESULTS AND DISCUSSION

Electrical Resistivities of PPS/MWCNT/PA6 Composites

PPS/1 wt % MWCNT/PA6 composites were firstly prepared using direct melt mixing where PPS, PA6, and MWCNTs were placed together in a rheometer and melt-mixed at 300°C for 8
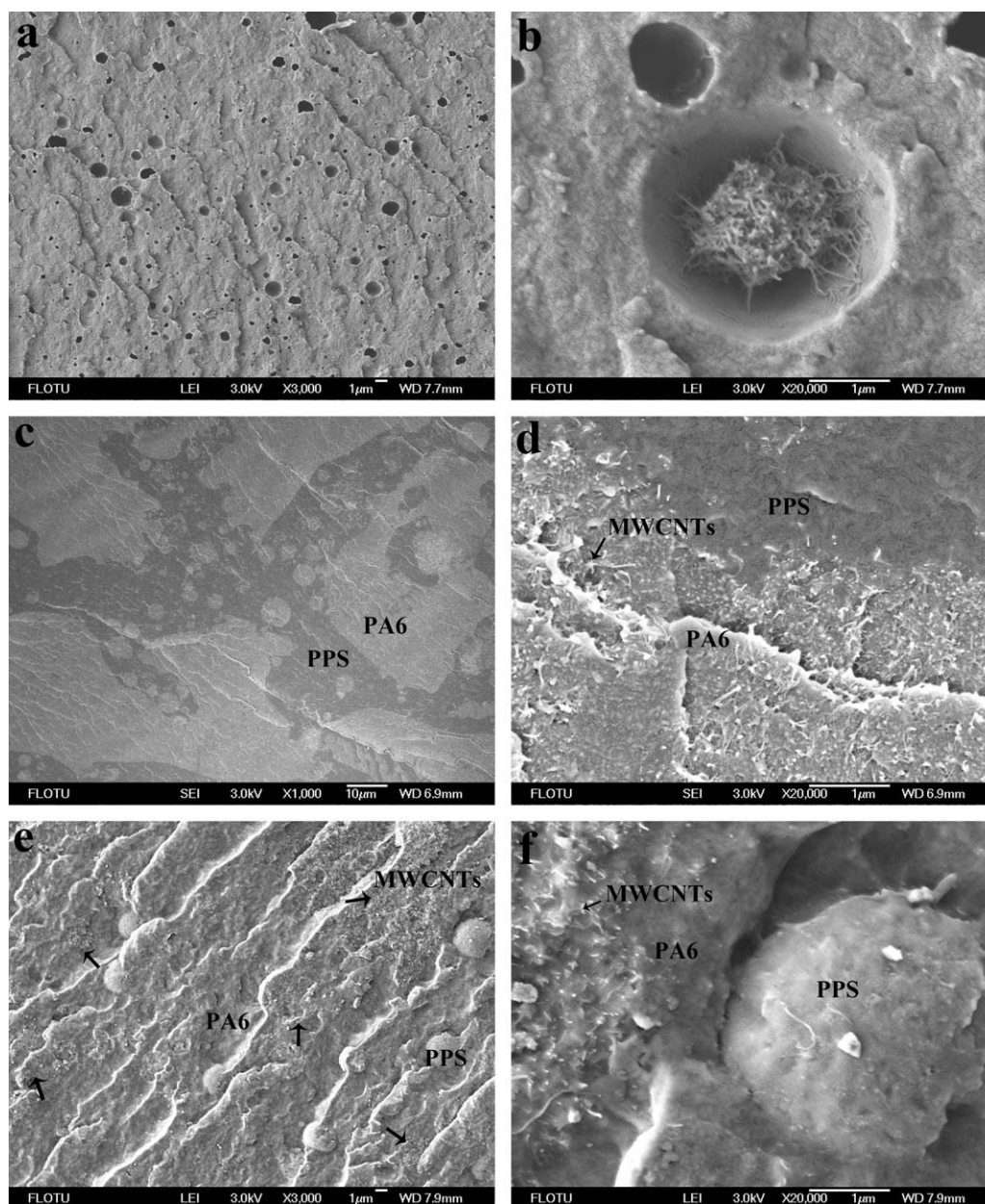
Figure 2. FESEM micrographs of cryo-fractured surfaces of PPS/1 wt % MWCNT/PA6-d composites with different PA6 contents: (**a, b**) 20 wt %, where the PA6 phases were removed by extraction with formic acid at room temperature for 20 min, (**c, d**) 50 wt %, and (**e, f**) 80 wt %.

min. The rotation rate was fixed at 60 rpm to get a balance between shear strength and mixing time to minimize the degradation of PA6, because both high shear strength and long mixing time could lead to serious degradation of PA6. As shown in Figure 1, PPS/1 wt % MWCNT composite is non-conductive with a very high electrical resistivity ($lg\rho_v \approx 17$). After the incorporation of 10–30 wt % PA6, the electrical resistivities of the composites slightly decrease, but are still high ($lg\rho_v = 9$–11). However, with 40–90 wt % PA6, the electrical resistivities of the composites are very low ($lg\rho_v \approx 3$) and the materials are conductive.

To obtain conductive composites with 10–30 wt % PA6, a masterbatch approach was then envisaged, where MWCNTs were

pre-compounded into the matrix polymer PPS in a high concentration. Thus, PPS/5 wt % MWCNT was diluted with PA6 and PPS at 300°C for 8 min, and the resulting composites are conductive with a $lg\rho_v$ of 3. The advantage of low incorporation of PA6 is minimum destruction on the heat resistance and mechanical properties of PPS. Therefore, conductive PPS/10–30 wt % PA6/MWCNT composites are promising materials.

Morphology of the Electrically Conductive Composites

Morphological investigation was performed with FESEM and TEM in order to understand the difference in electrical resistivities of the composites with different amounts of PA6 and with different methods. Figure 2 shows FESEM micrographs of PPS/1 wt % MWCNT/PA6-d composites having 20, 50, and 80 wt %
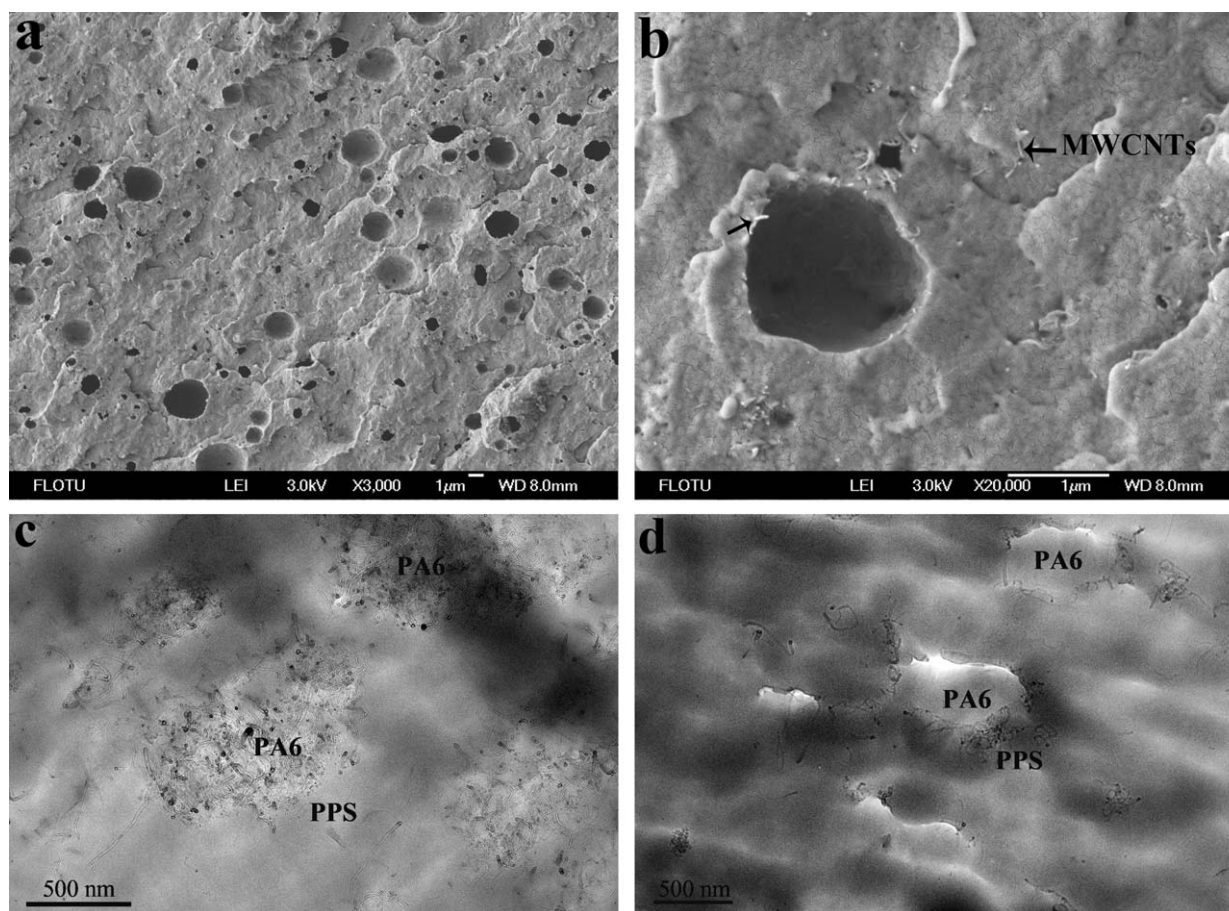
Figure 3. FESEM micrographs of PPS/1 wt % MWCNT/20 wt % PA6 composites: (**a, b**) PPS/1 wt % MWCNT/20 wt % PA6-m, where the PA6 phases were removed by formic acid at room temperature for 8 min, and TEM micrographs of PPS/1 wt % MWCNT/20 wt % PA6 composites: (**c**) PPS/1 wt % MWCNT/20 wt % PA6-d, and (**d**) PPS/1 wt % MWCNT/20 wt % PA6-m.

PA6. Most of MWCNTs are localized in the PA6 phase and at the interface between PA6 and PPS in all the composites. When PA6 is the minor component [20 wt %, Figure 2(a,b)], a typical sea-island structure is observed with PA6 as the dispersed phase and PPS as the matrix phase, and the conductive paths cannot be easily formed because most of MWCNTs are isolated in the

islands. It is noted that some of MWCNTs localized at the interface penetrate to the PPS matrix phase and there are indeed some MWCNTs in the PPS matrix phase although not many [Figure 3(c)], and these facilitate the formation of conductive paths. As a result of the combined actions of the above factors, the electrical resistivities decrease but the composites are still non-conductive.

With 50 wt % PA6 [Figure 2(c,d)], mixed structures are observed. It is mainly constructed with a co-continuous structure although some PA6 particles co-exist. The material is conductive because of the double percolation phenomenon, being in agreement with the literature reports.[1,7,8,13] When PA6 is the major component [80 wt %, Figure 2(e,f)], an inverse sea-island structure with PA6 as the matrix phase and PPS as the dispersed phase, is observed. The existence of PPS can increase the effective concentration of MWCNTs in PA6 phase, and thus facilitate the formation of conductive paths, similar to the cases of PC/SAN/MWCNT and PC/ABS/MWCNT composites.[6,22]

FESEM and TEM micrographs of PPS/1 wt % MWCNT/20 wt % PA6 composite prepared by the masterbatch approach are shown in Figure 3(a,b,d). MWCNTs are observed mainly in the PPS matrix phase and at the interface, being different from the case of direct melt mixing [Figure 3(c)]. The mechanism for the
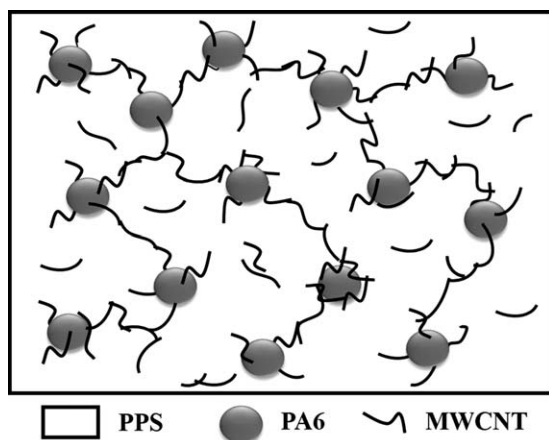
Figure 4. Illustration of co-supporting conductive networks in PPS/ MWCNT/PA6-m composites.

Table I. Contact Angles and Surface Tensions of PPS and PA6 Measured with Water and Diiodomethane

Samples	Average contact angle (°)		γ (20°C) (mN/m)	γ^d (20°C) (mN/m)	γ^p (20°C) (mN/m)
	Water	Diiodomethane			
PPS	96	38.6	40.5	40.3	0.2
PA6	72.5	37.8	46.7	40.7	6.0

Table II. Surface Tensions of Water, Diiodomethane, PPS, PA6, and MWCNTs

Samples	γ (20°C) (mN/m)	γ (300°C) (mN/m)	γ^d (300°C) (mN/m)	γ^p (300°C) (mN/m)	Ref.
Water	72.8	–	–	–	38
Diiodomethane	50.8	–	–	–	38
PPS	40.5	21.9	21.8	0.1	
PA6	46.7	25.2	22.0	3.2	
MWCNTs-1	45.3	45.3	18.4	26.9	36
MWCNTs-2	27.8	27.8	17.5	10.3	37

conduction is illustrated in Figure 4. There are two types of conductive fillers in the system: MWCNTs and PA6 particles surrounded by MWCNTs with some parts in the PPS phase. They form co-supporting conductive networks in which MWCNTs act as long distance charge transporters and PA6 particles serve as interconnections between MWCNTs, similar to the case of mixed carbon filler-filled polymers such as CB/MWCNT-filled PP[30] and graphite/CF-filled HDPE.[31]

Thermodynamic Prediction of the Localization of MWCNTs

Sumita's model is widely used to predict the distribution of fillers from thermodynamic viewpoint, which involves the calculation of the wetting coefficient ω_a based on Young's equation:[1]

$$\omega_a = \frac{\gamma_{A/MWCNT} - \gamma_{B/MWCNT}}{\gamma_{A/B}} \quad (3)$$

where $\gamma_{A/MWCNT}$ is the interfacial tension between component A and MWCNTs, $\gamma_{B/MWCNT}$ is the interfacial tension between component B and MWCNTs, and $\gamma_{A/B}$ is the interfacial tension between components A and B. When $\omega_a > 1$, MWCNTs locate into the B phase; When $\omega_a < -1$, MWCNTs distribute into the A phase; When $-1 < \omega_a < 1$, MWCNTs confine at the interface.

Before calculating, we used water and diiodomethane as two probe fluids to measure the contact angles of PPS and PA6, and then obtained their surface tensions at 20°C according to Owens

**Table III.** Interfacial Tensions Between Polymers and MWCNTs

| Samples	Temperature (°C)	Interfacial tension (mN/m, 300°C)
PPS/PA6	300	2.9
PPS/MWCNT-1	300	26.9
PA6/MWCNT-1	300	19.0
PPS/MWCNT-2	300	10.5
PA6/MWCNT-2	300	4.2

eqs. (1) and (2). The contact angles and surface tensions are listed in Table I.

At high temperature, the surface tensions of polymers can be calculated with the following two formulas:[32]

Table IV. Wetting Coefficients and Prediction for the Location of MWCNTs

Samples	Temperature (°C)	ω_a	Prediction for the localization of MWCNTs
PPS/PA6/MWCNT-1	300	2.7	PA6
PPS/PA6/MWCNT-2	300	2.2	PA6
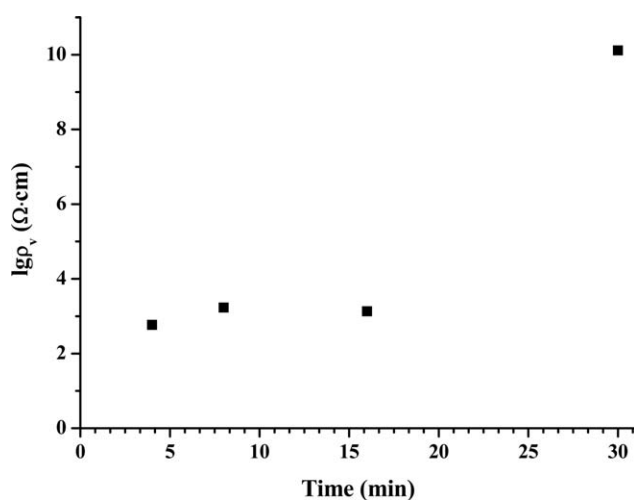
Figure 5. Electrical resistivity of PPS/1 wt % MWCNT/20 wt % PA6-m composite as a function of mixing time.
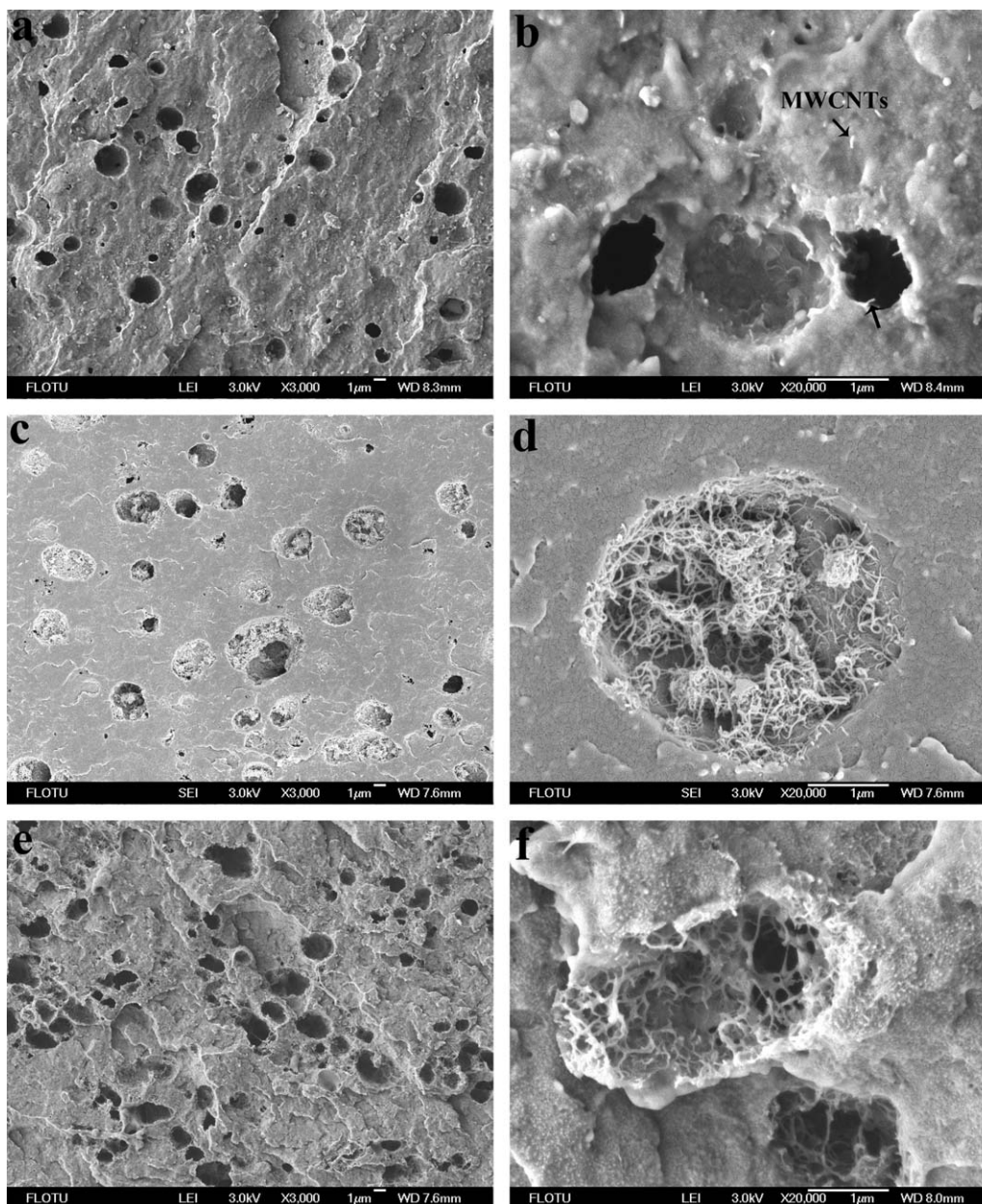
Figure 6. FESEM micrographs showing cross sections of PPS/1 wt % MWCNT/20 wt % PA6-m composites prepared with different mixing times: (**a, b**) 4 min, (**c, d**) 16 min, and (**e, f**) 30 min.

$$-\frac{d\gamma}{dT}=\frac{11}{9}\frac{\gamma_0}{T_c}\left(1-\frac{T}{T_c}\right)^{\frac{2}{9}} \tag{4}$$

$$\gamma=\gamma_0\left(1-\frac{T}{T_c}\right)^{\frac{11}{9}} \tag{5}$$

where γ_0 is surface tension of polymer at 0 K; T_c is the critical temperature, 1000 K for most polymers, and T is the mixing temperature, which is 573 K in our study. The values of the surface tensions of PPS and PA6 at 300°C calculated from eqs. (4) and (5) are showed in Table II. Two values of the surface tensions of MWCNTs from the literature[36,37] are also listed in Table II and used next to calculate the interfacial tension between each polymer and MWCNTs.

In general, the interfacial tensions between MWCNTs and each polymer (PPS or PA6) can be estimated by harmonic-mean eq. (6).[39]

$$\gamma_{A/B}=\gamma_A+\gamma_B-4\left(\frac{\gamma_A^d\gamma_B^d}{\gamma_A^d+\gamma_B^d}+\frac{\gamma_A^p\gamma_B^p}{\gamma_A^p+\gamma_B^p}\right) \tag{6}$$

where γ_A^d, γ_A^p, γ_B^d, γ_B^p are the dispersive and the polar parts of surface tensions of components A and B. The calculated values of interfacial tensions between polymers and MWCNTs are shown in Table III. The wetting coefficient ω_a (Table IV) is calculated by eq. (3), where A and B are corresponding to PPS and PA6 in the original formula, respectively. Since $\omega_a = 2.7 > 1$, the localization of MWCNTs is predicted in the
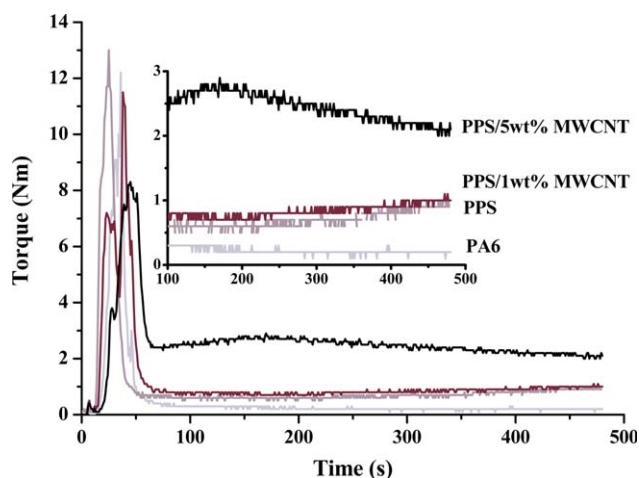
Figure 7. Torque-time curves for PA6, PPS, PPS/1 wt % MWCNT, and PPS/5 wt % MWCNT. [Color figure can be viewed in the online issue, which is available at wileyonlinelibrary.com.]

PA6 phase, which is in agreement with the situation of direct melt mixing.

Migration Kinetics of MWCNTs From Unfavored PPS to PA6 Phase

The actual localization of MWCNTs depends not only on thermodynamic but also on kinetic factors.[26,32] It is well-known that the processing temperature for PA6 (typically 240°C) is much lower than for PPS (typically 300°C). Therefore, PA6 melts earlier than PPS during melt mixing. In direct melt mixing, MWCNTs go into PA6 after the melting of PA6, and stay in the PA6 phase or at the interface after the melting of PPS and further mixing because PA6 is the thermodynamically favored phase. In the masterbatch approach, MWCNTs are precompounded into thermodynamically unfavored PPS, and the melt mixing process should involve migration of MWCNTs from PPS toward PA6. Whether or not one can obtain conductive composites depends on the migration rate of MWCNTs. If the migration of MWCNTs is too fast to control, then it is difficult to obtain conductive composites. On the contrary, if the migration process is slow enough, then conductive composites can be obtained by controlling the mixing time. In this work, conductive PPS/1 wt % MWCNT/10–30 wt % PA6 are obtained with the masterbatch approach by melt mixing for 8 min, revealing slow migration of MWCNTs. As a comparison, it has been reported that MWCNTs have already migrated from thermodynamically unfavored SAN to thermodynamically favored PC after 5 min of melt mixing.[23] In another report, most MWCNTs take only about 4 min to migrate from thermodynamically unfavored PLA to the interface of PLA/PCL.[7]

To know if MWCNTs can eventually migrate to the thermodynamically favored PA6 phase, the electrical resistivity and morphology of the PPS/1 wt % MWCNT/20 wt % PA6-m composite as a function of mixing time are investigated. As shown in Figure 5, the electrical resistivities of the composites prepared with 4, 8, and 16 min of mixing are low (lgρ_v around 3), and it increases dramatically after 30 min of mixing (lgρ_v around 10). FESEM micrographs showing the morphology of

the composites prepared with mixing time of 4, 16, and 30 min are shown in Figure 6. With 4 min of mixing, MWCNTs are mainly found in the PPS matrix phase and at the interface revealed by the protruded ends of MWCNTs in the holes generated after extraction of PA6 with formic acid. As mentioned earlier this type of morphology facilitates the formation of conductive paths because the PA6 particles surrounded by MWCNTs can act as big-sized conductive particles.

When the mixing time is prolonged to 16 min, most MWCNTs are observed at the interface with some parts still in the PPS phase, as evidenced by the presence of large amount of un-removed MWCNTs in the holes after the removal of PA6 particles, indicating that MWCNTs are migrating from PPS phase toward PA6 phase. The mechanism for the conduction is similar to that of the samples obtained at 4 and 8 min, although more MWCNTs have migrated to the interface.

When the mixing time is unusually long such as 30 min, most MWCNTs are localized in the PA6 phase and removed along with PA6 phase after extracting with formic acid. The observed MWCNTs localized at the interface which are not removed by formic acid are much less than in the case of 16 min, suggesting that a large amount of MWCNTs have already migrated to PA6 particles, and thus it is not surprising that the material becomes non-conductive.

From the above investigation, it can concluded that conductive PPS/1 wt % MWCNT/20 wt % PA6 can be obtained via PPS/5 wt % MWCNT masterbatch approach as long as the mixing time is less than 16 min. This is perfectly realistic in view of industrial production.

Discussion About the Slow Migration Rate of MWCNTs From PPS to PA6

It has been reported that the viscosity ratio of the two polymers in the blends has a significant (perhaps decisive) effect on the localization of CB and MWCNTs.[8,33,34] In general, the carbon fillers tend to localize in the low viscosity phase if the viscosity ratio of the two polymers is big. So far, only few examples are reported, and currently no general rule exists. In our case, the viscosity ratio of PPS/PA6 is quite big as evidenced by the equilibrium torque values shown in Figure 7. The equilibrium torque value of PPS/5 wt % MWCNT masterbatch is even much bigger than that of neat PPS. We think that the high viscosity ratio of PPS/PA6 or PPS/MWCNT masterbatch/PA6 could be an important reason for the slow migration rate of MWCNTs from PPS to PA6. It is reasonable to think that MWCNTs travel slowly in a highly viscous medium.

CONCLUSION

Conductive PPS/1 wt % MWCNT/10–30 wt % PA6 composites cannot be prepared by direct melt mixing because MWCNTs are mostly isolated in the PA6 islands and at the interface, but they can be prepared using PPS/5 wt % MWCNT masterbatch approach where most MWCNTs are localized in the thermodynamically unfavored PPS matrix phase and at the interface. The mechanism for the conduction is proposed by taking PA6 particles surrounded by MWCNTs with parts in the PPS phase as one type of conductive fillers, which along with MWCNTs localized in

the PPS matrix form co-supporting conductive networks in which MWCNTs act as long distance charge transporters and PA6 particles serve as interconnections between MWCNTs.

The migration kinetics shows that MWCNTs can eventually migrate into the PA6 phase after an unusually long mixing time (30 min), indicating the slow migration rate of MWCNTs in the masterbatch approach. This could be attributed to the high viscosity ratio of the two polymers, and can be used to prepare conductive MWCNT-filled PPS/PA6 blends.

ACKNOWLEDGMENTS

REFERENCES

1. Sumita, M.; Sakata, K.; Asai, S.; Miyasaka, K.; Nakagawa, H. *Polym. Bull.* **1991**, *25*, 265.

2. Sahoo, N. G.; Rana, S.; Cho, J. W.; Li, L.; Chan, S. H. *Prog. Polym. Sci.* **2010**, *35*, 837.

3. Deng, H.; Lin, L.; Ji, M. Z.; Zhang, S. M.; Yang, M. B.; Fu, Q. *Prog. Polym. Sci.* **2014**, *39*,627.

4. Shrivastava, N. K.; Suin, S.; Maiti, S.; Khatua, B. B. *RSC. Adv.* **2014**, *4*, 24584.

5. Fu, Y.; Liu, L. S.; Zhang, J. W. *ACS Appl. Mater. Interfaces* **2014**, *6*, 14069.

6. Göldel, A.; Kasaliwal, G.; Pötschke, P. *Macromol. Rapid. Commun.* **2009**, *30*, 423.

7. Huang, J. R.; Mao, C.; Zhu, Y. T.; Jiang, W.; Yang, X. D. *Carbon* **2014**, *73*, 267.

8. Shi, Y. Y.; Yang, J. H.; Huang, T.; Zhang, N.; Chen, C.; Wang, Y. *Compos. Part B* **2013**, *55*, 463.

9. Göldel, A.; Marmur, A.; Kasaliwal, G. R.; Pötschke, P.; Heinrich, G. *Macromolecules* **2011**, *44*, 6094.

10. Pötschke, P.; Bhattacharyya, A. R.; Janke, A. *Polymer* **2003**, *44*, 8061.

11. Mi, D.; Liu, K.; Du, H. N.; Zhang, J. *Polym. Adv. Technol.* **2014**, *25*, 364.

12. Farimani, H. E.; Ebrahimi, N. G. *J. Appl. Polym. Sci.* **2012**, *124*, 4598.

13. Mao, C.; Zhu, Y. T.; Jiang, W. *ACS Appl. Mater. Interfaces* **2012**, *4*, 5281.

14. Maiti, S.; Shrivastava, N. K.; Khatua, B. B. *Polym. Compos.* **2013**, *34*, 570.

15. Sun, Y.; Guo, Z. X.; Yu, J. *Macromol. Mater. Eng.* **2010**, *295*, 263.

16. Sun, Y.; Jia, M. Y.; Guo, Z. X.; Yu, J.; Nagai, S. *J. Appl. Polym. Sci.* **2011**, *120*, 3224.

17. Thongruang, W.; Balik, C. M.; Spontak, R. J. *J. Polym. Sci. Part B: Polym. Phys.* **2002**, *40*, 1010.

18. Koysuren, O.; Yesil, S.; Bayram, G. *J. Appl. Polym. Sci.* **2010**, *118*, 3041.

19. Xu, Z. B.; Zhao, C.; Fang, Z. P.; Tong, L. F. *J. Appl. Polym. Sci.* **2007**, *106*, 2008.

20. Al-Saleh, M. H.; Sundararai, U. *Compos. Part A* **2008**, *39*, 284.

21. Xiong, Z. Y.; Sun, Y.; Wang, L.; Guo, Z. X.; Yu, J. *Sci. China Chem.* **2012**, *55*, 808.

22. Xiong, Z. Y.; Wang, L.; Sun, Y.; Guo, Z. X.; Yu, J. *Polymer* **2013**, *54*, 447.

23. Pötschke, P.; Pegel, S.; Claes, M.; Bonduel, D. *Macromol. Rapid. Commun.* **2008**, *29*, 244.

24. Xiang, F. M.; Wu, J.; Liu, L.; Huang, T.; Wang, Y.; Cheng, C.; Peng, Y.; Jiang, C. X.; Zhou, Z. W. *Polym. Adv. Technol.* **2011**, *22*, 2533.

25. Gubbels, F.; Jérôme, R.; Teyssié, Ph.; Vanlathem, E.; Deltour, R.; Calderone, A.; Parenté, V.; Brédas, J. L. *Macromolecules* **1994**, *27*, 1972.

26. Gubbels, F.; Jérôme, R.; Vanlathem, E.; Deltour, R.; Blacher, S.; Brouers, F. *Chem. Mater.* **1998**, *10*, 1227.

27. Dai, K.; Xu, X. B.; Li, Z. M. *Polymer* **2007**, *48*, 849.

28. Baudouin, A. C.; Devaux, J.; Bailly, C. *Polymer* **2010**, *51*, 1341.

29. Liebscher, M.; Blais, M. O.; Pötschke, P.; Heinrich, G. *Polymer* **2013**, *54*, 5875.

30. Sun, Y.; Bao, H. D.; Guo, Z. X.; Yu, J. *Macromolecules* **2009**, *42*, 459.

31. Thongruang, W.; Spontak, R. J.; Balik, C. M. *Polymer* **2002**, *43*, 2279.

32. Fenouillot, P.; Cassagnau, J.; Majesté, J. C. *Polymer* **2009**, *50*, 1333.

33. Feng, J. Y.; Chan, C. M.; Li, J. X. *Polym. Eng. Sci.* **2003**, *43*, 1058.

34. Zonder, L.; Mccarthy, S.; Rios, F.; Ophir, A.; Kenig, S. *Adv. Polym. Technol.* **2014**, *33*, 21427.

35. Tavana, H.; Lam, C. N. C.; Grundke, K.; Friedel, P.; Kwok, D. Y.; Hair, M. L.; Neumann, A. W. *J. Colloid. Interface Sci.* **2004**, *279*, 493.

36. Nuriel, S.; Liu, L.; Barber, A. H.; Wagner, H. D. *Chem. Phys. Lett.* **2005**, *404*, 263.

37. Barber, A. H.; Cohen, S. R.; Wagner, H. D. *Phys. Rev. Lett.* **2004**, *92*, 186103.

38. Bialopiotrowicz, T. *Food Hydrocolloid* **2003**, *17*, 141.

39. Wu, S. Polymer Interface Adhesion; Marcel Dekker Inc: New York, **1982**.